Effect of Surfactant/Silica Molar Ratios on the Formation of Mesoporous Molecular Sieves: Inorganic Mimicry of Surfactant Liquid-Crystal Phases and Mechanistic Implications

J. C. Vartuli,*,† K. D. Schmitt,† C. T. Kresge,‡ W. J. Roth,‡ M. E. Leonowicz,‡
S. B. McCullen,† S. D. Hellring,† J. S. Beck,† J. L. Schlenker,† D. H. Olson,† and
E. W. Sheppard†

Mobil Research and Development Corporation, Central Research Laboratory,
Princeton, New Jersey 08543, and Paulsboro Research Laboratory,
Paulsboro, New Jersey 08066

Received April 15, 1994. Revised Manuscript Received August 15, 1994[®]

The influence of surfactant/silica molar ratio (Sur/Si) in the synthesis of the mesoporous molecular sieve materials (M41S) was studied in a simple ternary synthesis system containing tetraethylorthosilicate (TEOS), water, and the cetyltrimethylammonium (CTMA) cation at 100 °C. The resulting silicate materials were characterized by X-ray diffraction, ^{29}Si NMR, and FTIR. As the Sur/Si molar ratio increased from 0.5 to 2, the siliceous products obtained could be classified into four separate groups: MCM-41 (hexagonal), MCM-48 (cubic), thermally unstable M41S, and a molecular species, the cubic octamer $[(CTMA)SiO_{2.5}]_8$. One of the thermally unstable structures has been identified as a lamellar phase. These results are consistent with known micellar phase transformations that occur at various surfactant concentrations and reinforce the concept that liquid-crystal structures serve as templating agents for the formation of M41S type materials.

Introduction

The discovery of a new family of mesoporous molecular sieves (M41S) was recently reported by researchers at Mobil R&D Corp.[1] and has been the subject of several review articles.[2] M41S materials exhibit narrow pore size distributions, similar to those exhibited by zeolitic materials. However, the pore systems of M41S materials can be tailored with dimensions between 15 and 100 Å. High hydrocarbon sorption capacity and thermal stability are also attractive properties of these new molecular sieves. The M41S family contains several unique members, MCM-41, having a hexagonal arrangement of unidimensional pores, MCM-48, exhibiting cubic structure which can be indexed to an *Ia*3*d* unit cell, and other species whose structures have not yet been elucidated. M41S materials exist in a wide range of compositions and are synthesized hydrothermally in the presence of alkyltrimethylammonium surfactant cations having an alkyl side chain of greater than six carbon atoms.

As noted in our earlier work, the role of surfactant chemistry is critical for the formation of these materials.[1,3] Surfactant molecules have the ability to assemble into supramolecular arrays that form liquid-crystal structures. A liquid-crystal templating mechanism (LCT) in which surfactant liquid-crystal structures serve as organic templates (rather than single molecules commonly proposed as templates in zeolite synthesis) has been proposed for the formation of these M41S type materials.[1,3] Both the generation of varied pore size MCM-41 by either the use of different length surfactant molecules or by use of micellar solubilization techniques, and the existence of M41S materials having structures (hexagonal, cubic, and lamellar) that mimic known liquid-crystal phases strongly support this proposed mechanism. Two possible mechanistic pathways suggest either (A) the liquid-crystal phase may form prior to the addition of the reagents or (B) the silicate species generated in the reaction mixture may influence the ordering of surfactant micelles to the desired liquid crystal phase.[1,3]

For either pathway, the resultant composition would produce an inorganic material that mimics known liquid-crystal phases. For pathway A to be operative, it is required that the surfactant molecules exist in sufficient concentration for a liquid-crystal structure to form. This liquid-crystal structure serves as the templating agent and the inorganic silicate anions merely serve to counterbalance the charge of these fully ordered surfactant aggregates. For pathway B, surfactant is only part of the template. The presence of a silicate anion species not only serves to charge balance the surfactant cations but also participates in the formation and ordering of the liquid-crystal phase.

Surfactant literature data do not support pathway A, especially for the alkyltrimethylammonium cation system, since the presence of the various liquid-crystal structures appears unlikely at the concentrations used

---

† Mobil Research and Development Corp., Central Research Laboratory.

‡ Mobil Research and Development Corp., Paulsboro Research Laboratory.

® Abstract published in *Advance ACS Abstracts,* November 1, 1994.

(1) Kresge, C. T.; Leonowicz, M. E.; Roth, W. J.; Vartuli, J. C.; Beck, J. S. *Nature* **1992**, *359*, 710–712.

(2) Ozin, G. A. *Adv. Mater.* **1992**, *4* (10), 612–48. Behrens, P. *Adv. Mater.* **1993**, *5* (2), 127–32. Behrens, P.; Stucky, G. D. *Angew. Chem., Int. Ed. Engl.* **1993**, *32* (5), 696–99. Davis, M. E. *Nature* **1993**, *364*, 391–93.

(3) Beck, J. S.; Vartuli, J. C.; Roth, W. J.; Leonowicz, M. E.; Kresge, C. T.; Schmitt, K. D.; Chu, C. T.-W.; Olson, D. H.; Sheppard, E. W.; McCullen, S. B.; Higgins, J. B.; Schlenker, J. L. *J. Am. Chem. Soc.* **1992**, *114* (27), 10834–43.

0897-4756/94/2806-2317$04.50/0

to form M41S structures.[4] The synthesis data presented herein show that hexagonal, cubic, and lamellar M41S structures form by varying the silica concentration at constant surfactant concentration, thus implicating a more prominent role for the inorganic silicate anions.[3] It is these synthetic data that support pathway B and are the subject of this article.

Experimental Section

Materials. Tetraethylorthosilicate (TEOS), trimethylsilyl chloride, and hexamethyldisiloxane were obtained from Aldrich. Cetyltrimethylammonium chloride ($C_{16}H_{33}(CH_3)_3NCl$), 29 wt % aqueous solution, was obtained from Armak Chemicals. The $C_{16}H_{33}(CH_3)_3N^+OH/Cl^-$ solution was prepared by batch exchange of the 29% $C_{16}H_{33}(CH_3)_3NCl$ with IRA-400(OH) exchange resin, Rohm and Haas. The effective exchange of hydroxide for halide was ~30%. All chemicals were used as received.

Instrumentation. X-ray powder diffraction was obtained on a Scintag XDS 2000 diffractometer using Cu Kα radiation of wavelength 1.541 78 Å, a step size of 0.04° 2θ, a counting time per step of 10−100 s, and an energy-dispersive detector. Peak positions and peak amplitudes were obtained using a deconvolution algorithm supplied by Scintag. High-resolution transmission electron microscopy (TEM) images and electron diffraction patterns of microtomed sections were obtained on a JEOL 200 CX. Images from thin sections and thin grain edges were recorded under various focus conditions. Diffraction information from M41S materials is limited to relatively large *d* spacings, and the diffracted intensities are weak. Images show contrast reversal upon going through Gaussian focus, as expected from the appearance of the electron diffraction pattern. Furthermore, no reversal in image contrast is observed at large under focus conditions. These characteristics suggest that a weak phase object approximation is reasonable for the interpretation of these images. According to this interpretation, the light areas in the images correspond to a lack of scattering matter (pores), and the dark areas are concentrations of scattering matter (walls).

Benzene sorption data were obtained on a computer-controlled 990/951 DuPont TGA system. The calcined sample was dehydrated by heating at 350 or 500 °C to constant weight in flowing He. Benzene sorption isotherms were measured at 25 °C by blending a benzene saturated He gas stream with a pure He gas stream in the proper proportions to obtain the desired benzene partial pressure. Argon physisorption measurements were conducted on a physisorption apparatus as previously described.[5] The method of Horváth and Kawazoe[6] was used to determine pore diameters.

Si NMR spectra were obtained on a JEOL Tecmag 200 MHz NMR in 9.5 mm zirconia rotors at 39.64 MHz spinning 4−4.2 kHz using 90° pulses at 1200 s intervals with high-power proton decoupling. Between 36 and 72 pulses gave high-quality spectra. Air was used as the drive gas to obtain as much benefit as possible from O_2 paramagnetic relaxation.[7] TMS (tetramethylsilane) was used as shift standard.

Infrared spectral data were gathered using a Nicolet 7199 under a N_2 purge at 4 cm^{-1} resolution with an MCT-B detector. The samples were ground in KBr or polyethylene and pressed into thin wafers prior to analysis.

Synthesis. Tetraethylorthosilicate (TEOS) and the $C_{16}H_{33}(CH_3)_3N^+OH/Cl^-$ solution were combined in various proportions to give the appropriate surfactant to silica molar ratio (designated as Sur/Si ratio). No additional water was added to the syntheses. The two reactants were mixed for 1 h to allow the hydrolysis of the TEOS. In separate sets of experiments this hydrolysis step was conducted at both room temperature (~25 °C) and at ~4 °C. When the hydrolysis of the TEOS was conducted at ~4 °C, the products were similar to those obtained from the room-temperature hydrolysis experiments, but phase transformations took place at higher Sur/Si ratios. For example, the cubic structure was observed at ratios as high as 1.5 when the hydrolysis was conducted at 4 °C compared to approximately 1.0 for ambient temperature hydrolysis. The reasons for this effect are not apparent at this time, although it may be due to the variation in the concentration of silicate species as a function of the hydrolysis temperature. These mixtures were placed in polypropylene bottles and placed into a steam box (~100 °C) for 48 h. The caps of the polypropylene bottles containing the reactant mixtures were deliberately left loosely fastened in the steambox to allow for the evaporation of the ethanol produced in the hydrolysis of the TEOS. Any variation of product was attributed to the change in the surfactant/silica ratio. This ratio was varied between 0.5 and 2.

Table 1. Composition of Synthetic Mixtures for the Formation of Various M41S Phases

product	Sur/Si	TEOS/100 g of CTMAOH
MCM-41	0.6	30 g
MCM-48	1.0	20 g
lamellar	1.3	15 g
cubic octamer	1.9	10 g

The amounts of TEOS and CTMAOH solution used to synthesize examples of these four main groups of materials are shown in Table 1. The resultant products were recovered by filtration, washed in water, and air-dried at ambient temperature. The as-synthesized products were then calcined at 540 °C for 1 h in flowing nitrogen followed by 6 h in flowing air.

As the Sur/Si molar ratio was varied, the products formed could be grouped into four main categories: Sur/Si < 1 hexagonal (MCM-41), Sur/Si = 1−1.5, cubic (MCM-48), Sur/Si = 1.2−2, thermally unstable materials, and finally Sur/Si = 2 the cubic octamer, $[(CTMA)SiO)_{2.5}]_8$, is formed. The thermally unstable materials produce fairly well-defined X-ray diffraction (XRD) patterns in the as-synthesized form but upon calcination lost most, if not all, XRD definition. One of these thermally unstable species exhibited an XRD pattern consistent with a lamellar type structure (a common liquid-crystal phase).

The X-ray diffraction pattern of the as-synthesized MCM-41 material exhibited a high-intensity peak having a *d* spacing of approximately 40 Å and several higher angle peaks having *d* spacings consistent with hexagonal indexing of *hk*0 reflections. X-ray diffraction of the calcined MCM-41 revealed a high intensity first peak having a *d* spacing of approximately 34 Å (representing a lattice contraction after calcination of about 5 Å, $(6 \times \sqrt{3})/2$) and other peaks consistent with hexagonal *hk*0 indexing. The lattice contraction for MCM-41 materials varied depending on synthesis conditions. The X-ray diffraction pattern of the calcined material is shown in Figure 1a. Found in the as-synthesized product (wt %): C, 47.5; N, 2.29; Si, 15.3; ash (1000 °C), 32.0.

The X-ray diffraction pattern of the as-synthesized MCM-48 exhibited a high-intensity peak having a *d* spacing of approximately 39 Å and several higher angle peaks having *d* spacings consistent with cubic indexing. X-ray diffraction pattern of the calcined version revealed a high intensity first peak having a *d* spacing of approximately 33 Å (representing a lattice contraction after calcination of about 14 Å) and several peaks having *d* spacings with retention of the cubic indexing. The X-ray diffraction pattern of the calcined product is shown in Figure 1b. Found in the as-synthesized product (wt %): C, 33.4; N, 1.88; Si, 11.7; ash (1000 °C), 25.9.

The X-ray diffraction pattern of the as-synthesized lamellar material exhibited a high intensity peak having *d* spacings of approximately 36 Å and two higher angle peaks having *d* spacings (18 and 12 Å) consistent with lamellar indexing of

---

(4) Reiss-Husson, F.; Luzzati, V. *J. Phys. Chem.* **1964**, *68* (12), 3504−11.

(5) Borghard, W. S.; Sheppard, E. W.; Schoennagel, H. J. *Rev. Sci. Instrum.* **1991**, *62*, 2801−2809.

(6) Horváth, G.; Kawazoe, K. *J. Chem. Eng. Jpn.* **1983**, *16* (6), 470−475.

(7) Cookson, D. J.; Smith, B. E. *J. Magn. Reson.* **1985**, *63*, 217−218. Klinowski, J.; Carpenter, T. A.; Thomas, J. M. *J. Chem. Soc., Chem. Commun.* **1986**, 956−958.

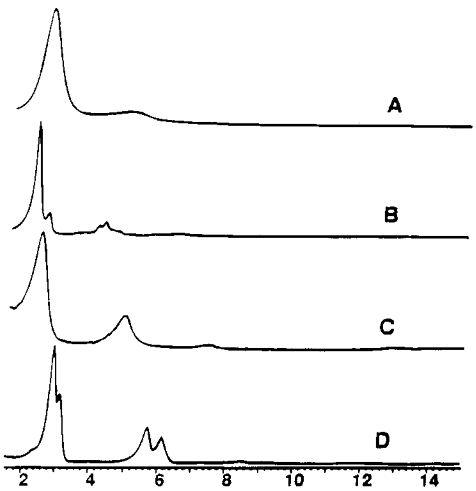

Figure 1. X-ray diffraction patterns of (A) calcined MCM-41, (B) calcined MCM-48, (C) as-synthesized lamellar material, and (D) cubic octamer.

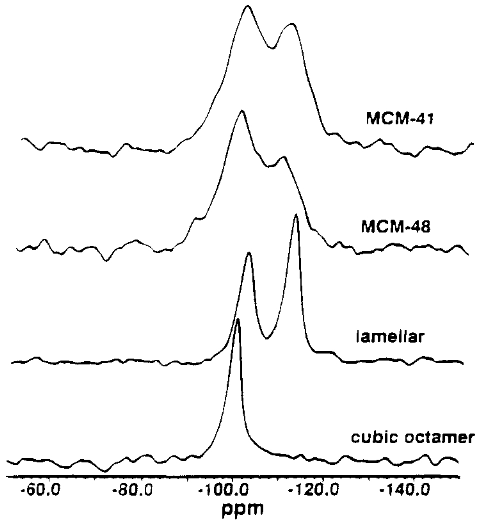

Figure 2. ^{29}Si NMR data of various Sur/Si products: (A) calcined MCM-41 (B), calcined MCM-48, (C) as-synthesized lamellar material, and (D) cubic octamer.

Table 2. ^{29}Si NMR Data for As-Synthesized Products

	chemical shift			mole %		
type	Q2	Q3	Q4	Q2	Q3	Q4
MCM-41	−89.1	−98.2	−108.0	8	49	43
MCM-48	−89.1	−98.2	−108.0	8	54	38
lamellar		−101.0	−111.1		52	48
octamer		−99.8			100	

00*l* reflections as shown in Figure 1c. Upon calcination at 540 °C the X-ray diffraction pattern was featureless. Found in the as-synthesized product (wt %): C, 45.1; N, 2.24; Si, 14.4; ash (1000 °C), 30.8.

The X-ray diffraction pattern of the as-synthesized cubic octamer material is shown in Figure 1d. After calcination at 540 °C, the X-ray diffraction pattern was featureless indicating that this material is unstable to this thermal treatment. Found in the as-synthesized product (wt %): C, 53.8; N, 2.76; Si, 6.8; ash (1000 °C), 14.2.

As is the case for the synthesis of MCM-41, MCM-48 and the lamellar material can be prepared from various alkyltrimethylammonium cations systems and under a variety of synthetic conditions. These factors will affect both the pore size of the product and the relative location of the peaks in the XRD pattern.

Trimethylsilylation. In a typical experiment, 0.50 g of sample, 10 g of trimethylsilyl chloride (TMSCl), and 15 g of hexamethyldisiloxane (HMDS) were refluxed overnight with magnetic stirring under N_2. The volatiles were stripped on a rotary evaporator, and the dry powder was washed two or three times with 10 mL of reagent grade acetone with centrifuging. Material recovery was typically >98%.

The trimethylsilylated silicate octamer, Q8M8, was prepared by adding, in order, 200 mL of DMF, 100 mL of HMDS, and 50 mL of TMSCl to 10 g of the organic silicate octamer in an Erlenmeyer flask and stirring magnetically for 20 min. The mixture was diluted with 200 mL of pentane, 100 mL of H_2O was added, the layers were separated, the organic was washed with another 50 mL of H_2O, the organic was stripped, the solid was taken up into 200 mL of cyclohexane, filtered and the product crystallized by slow evaporation of the solvent to give 3.16 g (97% yield) of waxy, white solid.

Results and Discussion

The X-ray diffraction and NMR data were used to establish the presence of four primary synthetic products. We first describe the general NMR data, then address in further detail the characterization of the individual materials, and finally discuss how these results support a silicate-initiated mechanistic pathway.

General NMR Data. Solid-state MAS Si NMR of the four primary as-synthesized materials is summarized in Figure 2 and Table 2. The spectra could be sorted into those with three overlapping broad peaks (hexagonal or cubic phases), two peaks (lamellar), and one peak (the cubic octamer). MCM-41 and MCM-48 have essentially the same ^{29}Si NMR spectra as amorphous silica. They show three broad peaks from Q4, Q3, and Q2 silicons (framework, silanol, disilanol). The peaks are broad, reflecting a wide range of Si−O−Si bond angles. The shifts and intensities were obtained by deconvolution.

In this synthesis system, as the Sur/Si increases, Q3 remains about the same ($\sim$50%) from MCM-41, MCM-48, and the lamellar material and increases to 100 mol % for the octamer. However, the Q3 content can vary depending on the synthesis conditions. The chemical analyses of the as-synthesized products are consistent with the invarient Q3 content. The N/Si molar ratio (initially assumed to represent the Q3 content) shows no variation with changes in the Sur/Si charge for the MCM-41, MCM-48, and lamellar products. Except for the octamer, the N/Si ratio remains unchanged at $\sim$0.30. For the octamer, the N/Si ratio was 0.81 where the expected value should be 1.00. The lack of agreement in the absolute numbers, Q3 (50%) and the N/Si ratios (30%), may indicate that some of the Q3 are not associated with the surfactant and may represent silanols or silanol nests formed in areas of incomplete silica condensation.

Characterization of the Individual Synthesized Materials

Hexagonal MCM-41. MCM-41 has been characterized previously.[3] Generally, MCM-41 exhibits an XRD pattern containing three or more low-angle peaks that can be indexed to a hexagonal *hk*0 pattern. MCM-41 characteristically exhibits a hydrocarbon sorption capacity of 0.7 mL/g or greater and the sorption isotherm contains a sharp inflection at a p/p_0, dependent on the pore size of the MCM-41, suggesting a uniform size pore system. Argon physisorption data confirm this narrow

Table 3. X-ray Diffraction Peaks and Cell-Parameter Refinement for Calcined Cubic MCM-48[a]

peak	index	2Θ	calculated 2θ	Δ2θ	rel intensity
1	211	2.670	2.669	0.001	100.0
2	220	3.085	3.081	0.004	12.3
3	321	4.066	4.077	−0.011	1.2
4	400	4.353	4.358	−0.005	1.1
5	420	4.874	4.873	0.001	3.8
6	332	5.109	5.111	−0.002	6.0
7	422	5.349	5.338	0.001	2.3
8	431	5.560	5.557	0.003	1.6

[a] a_0 (unit cell) = 81.09 (5) Å. (The quantity in parentheses is an estimated standard deviation (esd). This parameter is a measure of precision, not accuracy.)

pore size distribution. Depending on synthetic conditions, MCM-41 can be prepared with pore sizes ranging from ~15 to 100 Å.

Cubic MCM-48. X-ray Diffraction. A total of eight peaks were used to index the X-ray diffraction pattern of the calcined sample. The data and the results of this refinement in which all eight of the observed reflections were accounted for are shown in Table 3.

Comparison of the *d* spacings observed in this refinement yields a good correspondence to those predicted by the cubic *Ia3d* phase known in the surfactant literature. The calculated unit cell parameters, ~80 Å for the calcined MCM-48 sample were somewhat smaller than those observed, ~99 Å, for the cetyltrimethylammonium bromide "oil in water" *Ia3d* cubic analog.[8] However, this difference may reflect the shrinkage of the unit cell upon calcination due to further condensation of the silicate lattice. The cell parameter agreement is better for the as-synthesized MCM-48 material having an ~95 Å unit cell. A more systematic approach was applied to indexing the X-ray powder diffraction pattern of calcined MCM-48 preparation using a procedure developed by Bloss.[9] This procedure is applicable only to crystals belonging to the cubic crystal system. It was found that the XRD powder pattern of calcined MCM-48 could be indexed completely on the basis of a unit cell with $a = 81.09$ (5) Å. The observed reflections (Table 2) suggest systematic absences consistent with the uniquely determinable space group *Ia3d* ($I = h + k + l$, for hkl; and with h,k,l permutable k, $(l) = 2n$ for $0kl$ and $2h + l = 4n$ and ($l = 2n$) for hhl).[10,11] This assignment also matches crystallographic work on cubic lytropic crystal phases.

Argon Physisorption. Argon physisorption isotherms (Figure 3) were obtained over 0–0.9p/p_0 using an in-house physisorption apparatus.[5] The pore size of MCM-48, determined by the Horváth–Kawazoe method, was 28 Å (Figure 4). The pore volume was calculated to be approximately 0.60 cm^3/g similar to that obtained from MCM-41 samples having similar pore sizes.

Benzene Sorption. The benzene sorption isotherm of MCM-48 is shown in Figure 5. The isotherm exhibits a sharp inflection characteristic of capillary condensation within uniform pores, where the p/p_0 position of the inflection point is related to the diameter of the pore.[12,13] These characteristics were noted for MCM-41.[3] The p/p_0 of the inflection point for the MCM-48 sample is essentially the same as that for a MCM-41 sample prepared using the dodecyltrimethylammonium cation/TEOS system. These data are consistent with the pore size determination results by argon physisorption reported above.

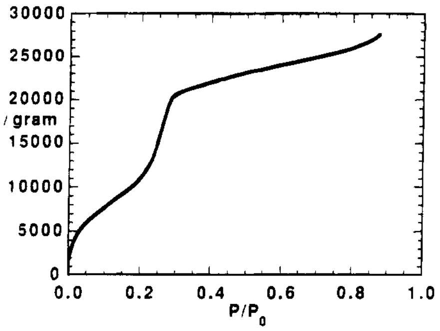

Figure 3. Argon physisorption isotherm of calcined MCM-48.

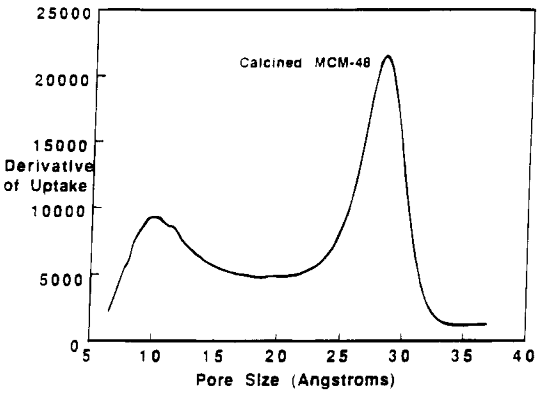

Figure 4. Horváth–Kawazoe argon physisorption plot of calcined MCM-48.

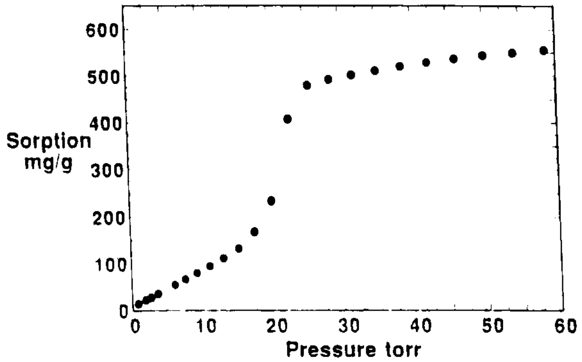

Figure 5. Benzene sorption data of calcined MCM-48.

Transmission Electron Microscopy. Transmission electron micrographs of thin sections of calcined MCM-48 (Figure 6) contain roughly circular regions that are about 1000–2000 Å in diameter. They usually display regular lattice fringes. A variety of two-dimensional lattice fringe patterns is observed in these micrographs, while samples of MCM-41 usually only give its characteristic hexagonal fringe pattern in

---

(8) Fontell, K. *Colloid Polym. Sci.* **1990**, *268*, 264–285.

(9) Bloss, F. D. *Crystallography and Crystal Chemistry*; Holt, Rinehart, and Winston: New York, 1971; pp 480–482.

(10) *International Tables for Crystallography*; Theo Hahn, Ed.; D. Reidel Publishing Co.: Dordrecht, Holland, 1983; Vol. A, Space-Group Symmetry, p 47.

(11) In ref. 10, p 706.

(12) Gregg, S. J.; Sing, K. S. W. *Adsorption, Surface Area, and Porosity*, 2nd ed.; Academic Press, Inc.: New York, 1982.

(13) Kerr, G. T.; Chester, A. W. *Thermochim. Acta* **1971**, *3*, 113–124.

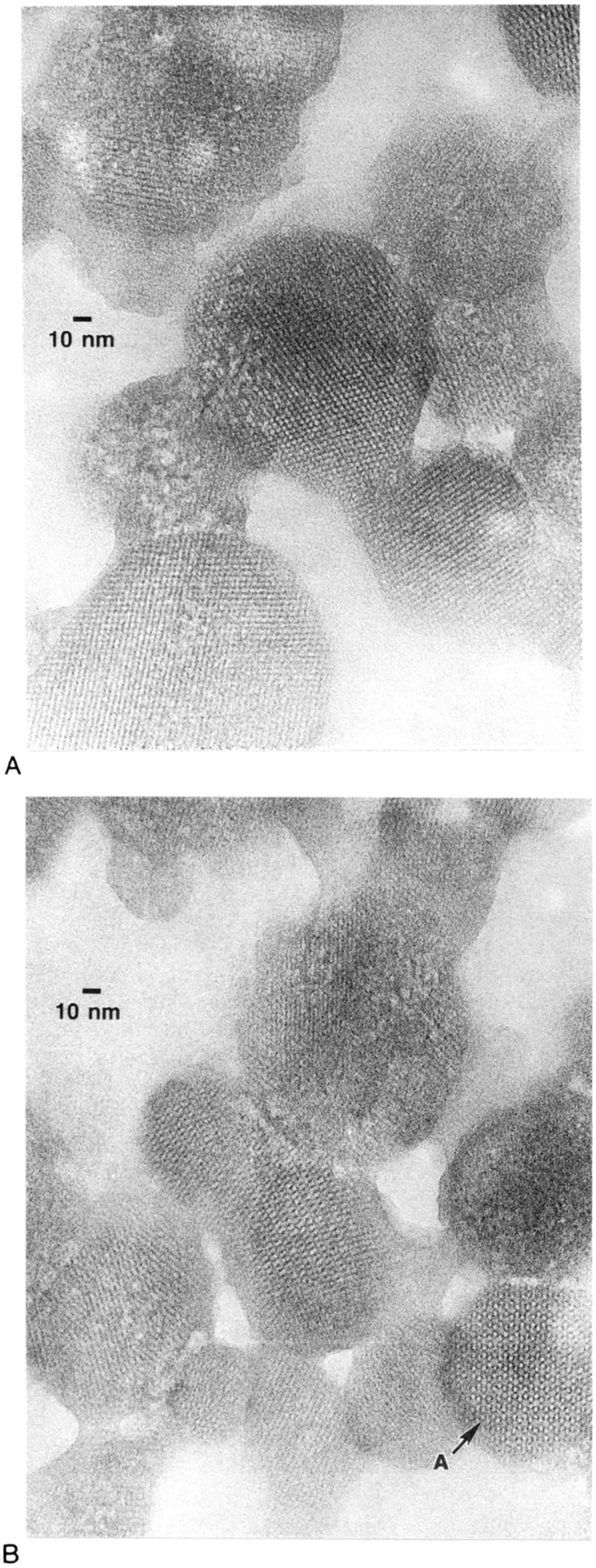

Figure 6. Transmission electron micrographs of MCM-48.

selected parts of the specimen that happen to be correctly aligned in the *hk*0 projection. The frequency and diversity of fringe patterns suggest that MCM-48 possesses observable three-dimensional order in more than one projection as expected for an analog of the cubic *Ia*3*d* liquid-crystal phase. One particularly interesting image is identified in Figure 6b as feature A. This unique pattern is believed to be the [111] projection of MCM-48.

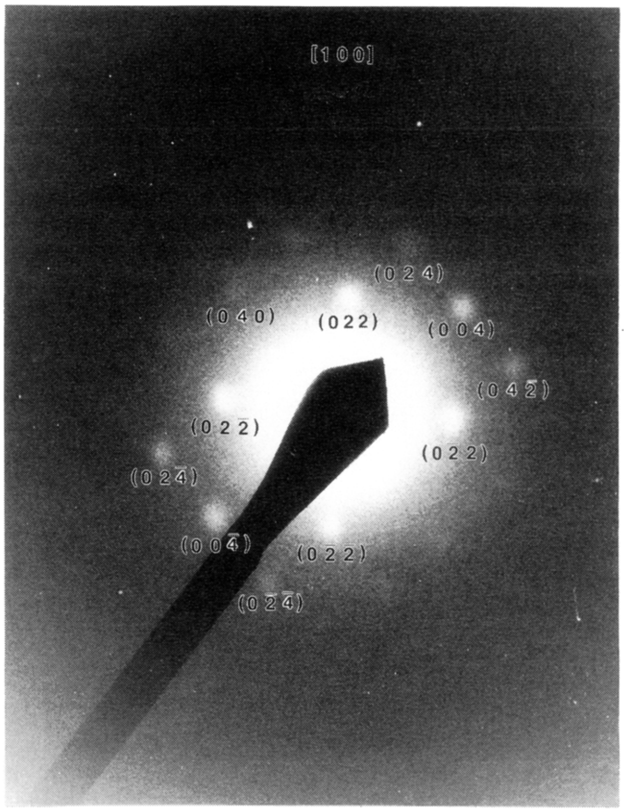

Figure 7. Indexed electron diffraction pattern of MCM-48 showing the [100] projection.

Figure 7 shows an indexed electron diffraction pattern of MCM-48. As expected, the pattern contains only a few diffraction maxima at large *d* spacings. Furthermore, the pattern contains some extraneous spots, indicating that more than one individual crystallite contributed to the electron diffraction pattern. It is reasonable to expect multiple crystal electron diffraction patterns from materials with such small crystal morphologies. Nevertheless, this pattern can be satisfactorily indexed (see Figure 7) as the [100] projection of the cubic *Ia*3*d* phase.

NMR and Silylation Results. The Si NMR spectra in both the as-synthesized and calcined forms of MCM-48 are unexceptional, showing a single broad peak centered at about -110 ppm. The spectra are not substantially different from those of MCM-41 or amorphous silicas. The Si NMR of trimethylsilyl derivatives from both the as-synthesized and calcined forms show narrowing due to conversion of the silanol in Q3 silicons to Q4 silicons by the trimethylsilyl chloride and the appearance of Me_3SiO peak(s) at 14 ppm. Integration showed roughly 16% of the silicons to be silanols in the as-synthesized form. This concentration is 0.67 mequiv/g, roughly half the 1.34 (N analysis)$-$1.46 mequiv/g (C analysis) of the template. This ratio was one-to-one for MCM-41. Whether this result is due to condensation of some silanols during synthesis or incomplete derivatization by trimethylsilyl chloride is unknown.

Silylation studies of both as-synthesized and calcined forms of MCM-48 produced rather surprising results. The treatment of the as-synthesized MCM-48 with TMSCl resulted in removal of the organic component

Table 4. Argon Physisorption Data for MCM-48 and the Silylated Products

sample	unit cell, Å	argon physisorption data	
		pore diam, Å	pore vol, mL/g
MCM-48 (as synthesized)	95		
organic extracted/silylated[a]	92	34	0.451
organic extracted/silylated[a]	92	34	0.405
MCM-48 (calcined)	81	28	0.608
calcined/silylated	80	26	0.591

[a] Replicate argon physisorption determinations.

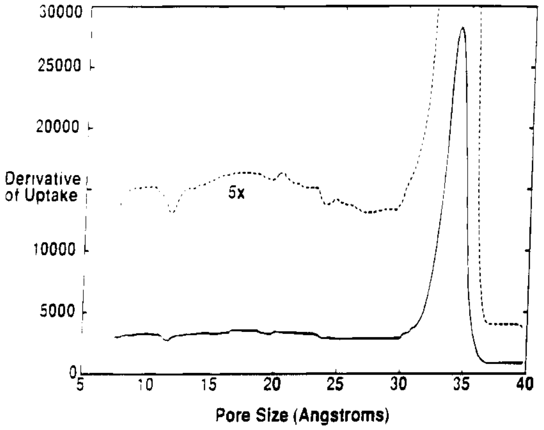

Figure 8. Horváth–Kawazoe argon physisorption plot of silylated MCM-48 from the as-synthesized form.

yielding a porous material with an average pore dimension of 34 Å (Table 4). This was accompanied by a moderate unit cell contraction of about 3 Å. In comparison, removal of the organic by calcination produced a unit-cell contraction of approximately 14 Å and a resultant pore size of about 28 Å. It would appear that the silylation of the silanol groups of MCM-48 (in the as-synthesized form) retarded this unit-cell contraction by removing available sites for silicate condensation. However, in view of the above trend it is difficult to explain why the silylated MCM-48 material with pore openings of 34 Å has a smaller void volume (~0.40–0.45 mL/g) than the 28 Å pore calcined material (~0.6 mL/g).

Figure 8 shows that the argon physisorption of the TMS-treated as-synthesized MCM-48 is unlike any large pore material examined thus far in that it shows no detectable monolayer sorption. The absence of the monolayer sorption peak is puzzling since no TMS-treated MCM-41 showed any such anomalous behavior. The TMS-treated MCM-41 samples showed the 9–10 Å monolayer peak and a decrease in pore volume that correlated quantitatively with the decrease in Horváth–Kawazoe pore diameter.[3]

The silylation of calcined MCM-48 produced only minimal changes in both pore size (from 28 to 26 Å) and void volume (from 0.61 to 0.59 mL/g). This final pore volume, however, is substantially more than that expected (~0.50 mL/g) if silylation reduced the pore diameter as noted for MCM-41 type materials.[3] Figure 9 shows the argon physisorption results for calcined MCM-48 sample and its TMS derivative with the x axis in the Horváth–Kawazoe transform. As expected, the results from the two samples illustrated in Figure 9 show the monolayer peak at 9–10 Å and the pore filling peak at 26 and 28 Å. The monolayer coverage accounts for about 24% of the total pore volume.

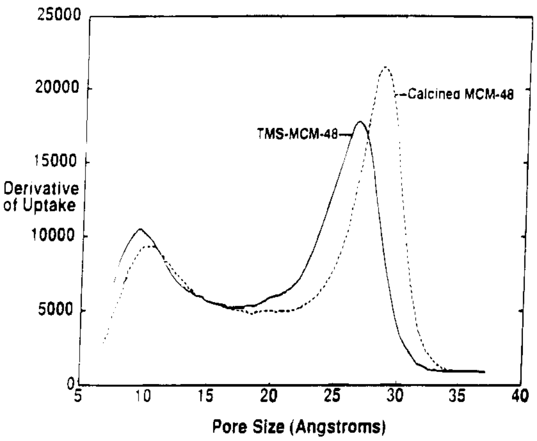

Figure 9. Horváth–Kawazoe argon physisorption plots of calcined MCM-48 and the silylated calcined version.

Structure Considerations. It has been proposed that the individual pores of MCM-41 are obtained from separate cylindrical micelles, while the ordered porous structure results from the hexagonal arrangement of this micellar array.[1,3] The structure of MCM-48 presents a significantly more complex problem than in the case of hexagonal MCM-41. The structure for MCM-48 is expected to be analogous to that of a liquid crystal with the cubic *Ia*3*d* symmetry, which has not been unequivocally elucidated. Over the years several models for the liquid crystal phase have been put forward. The proposed liquid-crystal structures include compositions with various orderings of (1) spherical, (2) cylindrical shaped micelles, or (3) a more complex system based on a bilayer aggregate that forms an infinite periodic minimal surface.[8,14–18] All three model systems can be indexed on a body-centered cubic lattice. The surfactant aggregate that forms the basis of the packed spherical model is a micellar sphere. For cylindrical ordering models, the cylindrical micelle is the basic unit. The infinite periodic minimal surface structure model uses bilayers of surfactant molecules, as shown in Figure 10. MCM-48 materials corresponding to any of the three proposed liquid-crystal structure models could contain a multidimensional pore system. A liquid-crystal template consisting of ordered spherical micelles forming MCM-48 could be easily visualized (Figure 10). For discrete surfactant micelles, the hydrophilic ends of the surfactant molecule make up the outer surface of the sphere, while the hydrophobic part of the surfactant molecule resides in the inside. A cubic packing of spherical micelles can be used to produce an inorganic structure (after removal of the surfactant molecules) with a three-dimensional pore system similar to that of zeolite A, for example. However, the aggregation of micellar spheres for the formation of the cubic structure has been generally discounted.[19]

The sequence of phases in a phase diagram precludes neither cylindrical micelles nor surfactant bilayers from consideration as the building units for the cubic phase

---

(14) Fontell, K. *J. Colloid Interface Sci.* **1972**, *43* (1), 156–164.

(15) Tiddy, G. J. T. *Phys. Rep.* **1980**, *57* (1), 1–46.

(16) Ekwall, P.; Mandell, L.; Fontell, K. *J. Colloid Interface Sci.* **1969**, *29* (4), 639–646.

(17) Larsson, L. *J. Phys. Chem.* **1989**, *93*, 7304–14.

(18) Charvolin, J.; Sadoc, J. F. *Colloid Polym. Sci.* **1990**, *268*, 190–95.

(19) Luzzati, V.; Spegt, P. A. *Nature* **1967**, *215*, 701–804.

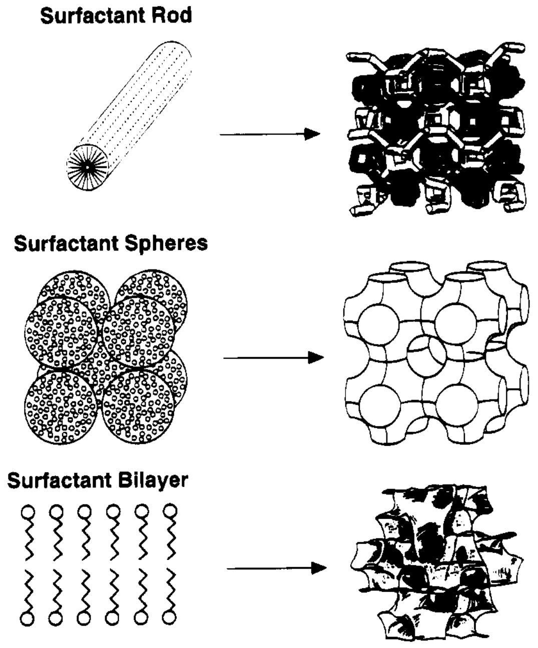

Figure 10. Possible surfactant micellar structures for the MCM-48 template.

since a phase transformation from hexagonal to cubic symmetry using cylindrical micelles is as conceivable as a transformation from the lamellar to cubic symmetry using a surfactant bilayer. The model which is currently most widely cited is a bicontinuous structure that has evolved from the proposal made by Luzzati.[20] The original simplified representation of the structure invoked two infinite three-dimensional, mutually intertwined, unconnected networks of rods made up by one of the components (either amphiphile or solvent). The other component occupied the space in between. The more sophisticated and apparently more realistic representation of this model is based on the concept of infinite periodic minimal surfaces. However, this interpretation is not shared by all the researchers in this field. Fontell differentiates between these two structures and assigns them to different *Ia*3*d* systems.[21] This controversy seems to indicate that the differences between the two structures are subtle and the problem may not be easily resolved. Additional experimental data that supports a bicontinuous structure for MCM-48 come from two sources: NMR data on the diffusion of water within the liquid-crystal phase[22,23] and the synthesis of a hydrocarbon polymer in the oil part of the cubic phase.[24] Fontell studied the diffusion coefficients of water, hydrocarbon, and surfactant in the systems didodecyldimethylammonium bromide/hydrocarbon/water[22] and monoglyceride/water.[23] He determined that the diffusion coefficients of water, hydrocarbon, and surfactant in the cubic phase were approximately the same as those in the lamellar phase and concluded that the micelle aggregate of the cubic and lamellar phase was the same.

A recent European patent application[24] claims the formation of a hydrocarbon polymer based porous material using the cubic phase of the didodecyldimethylammonium bromide/decane/water system as a template. The polymer product was indexed on a *Ia*3*d* lattice. This material presumably was formed within the hydrocarbon portion (oil phase) of the liquid-crystal phase, where MCM-48 is formed within the solvent portion (water phase). The ability to form equivalent *Ia*3*d* porous solids by polymerization in either the oil or water parts of the cubic liquid-crystal phase implies a bicontinuous structure.

A proposed bicontinuous structure for MCM-48 is consistent with the recent work of Monnier et al.[25] They were able to index the XRD pattern of MCM-48 to that predicted for the gyroid form of an infinite periodic minimal surface model (Q^{230}) proposed by Mariani.[26]

Lamellar Phase. The identities of all of the unstable phases formed at Sur/Si of $\sim$1.2–1.8 are not easily elucidated. The unstable phase described above has a characteristic XRD pattern (of the as-synthesized product) of well defined peaks (two or more) that are orders of the initial peak, suggesting some sort of ordered or layered material. This material was unstable when calcined. Lamellar products in surfactant containing syntheses have been suggested.

The unstable TEOS-based lamellar phase may not have thermal stability but it does appear to have crystalline structure. It shows two relatively sharp peaks for Q4 and Q3 silicons in 1:1 ratio in its Si NMR spectrum. The sharpness of these peaks suggests a repeating structure. On removal of template by calcination both the XRD and NMR fine structure disappear, but this is not the case for the silylated version. On treatment of as-synthesized material with TMSCl in HMDS/DMF, 33% of the solid (ash = 64% by TGA) was recovered as a water soluble salt. This material is CTMACl as identified by its C NMR spectrum. The remaining 60% had a Si NMR virtually unchanged from the as-synthesized material, that is, two sharp peaks at −100.9 and −110.5 ppm in 1:1 ratio. The structure was not affected by this treatment, nor was more than trivial trimethylsilylation accomplished. The NMR spectra of magadiite, a known layered silicate (Figure 11) are similar. The only difference is that the percentage of Q3 is higher for the surfactant–TEOS lamellar phase. For magadiite the Q3:Q4 ratio is approximately 35:65, whereas the TEOS lamellar product has a ratio of approximately 50:50 (by peak area). The synthesis temperature for magadiite ($\sim$175 °C) is higher than that of the TEOS-based lamellar material (100 °C). The higher Q3 content of the TEOS-based product indicates less polymerization of the silicon network. The broadness of the Q3 and Q4 peaks of the surfactant-based lamellar products relative to that of magadiite also suggests less regularity of the silicon structure.

The lamellar phase could be represented by sheets or bilayers of surfactant molecules with the hydrophilic ends pointed toward the oil–water interface, while the

---

(20) Luzzati, V.; Tardieu, A.; Gulik-Krzywicki, T.; Rivas, E.; Reiss-Husson, F. *Nature* **1968**, *220*, 485–88.

(21) Fontell, K. *Adv. Colloid Interface Sci.* **1992**, *41*, 127–47.

(22) Fontell, K.; Jansson, M. *Prog. Colloid Polym. Sci.* **1988**, *76*, 169–75.

(23) Lindblom, G.; Larsson, K.; Johansson, L.; Fontell, K.; Forsen, S. *J. Am. Chem. Soc.* **1979**, *101* (9), 5465–70.

(24) Anderson, D. European Patent Application, WO 90/07575, July 12, 1990.

(25) Monnier, A.; Schüth, F.; Huo, Q.; Kumar, D.; Margolese, D.; Maxwell, R. S.; Stucky, G. D.; Kishnamurthy, M.; Petroff, P.; Firouzi, A.; Janicke, M.; Chmelka, B. F. *Science* **1993**, *261*, 1299–1303.

(26) Mariani, P.; Luzzati, V.; Delacroix, H. *J. Mol. Biol.* **1988**, *204*, 165–89.

(27) Sprung, R.; Davis, M. E.; Kauffman, J. S.; Dybowski, C. *Ind. Eng. Chem. Res.* **1990**, *29*, 213–20.

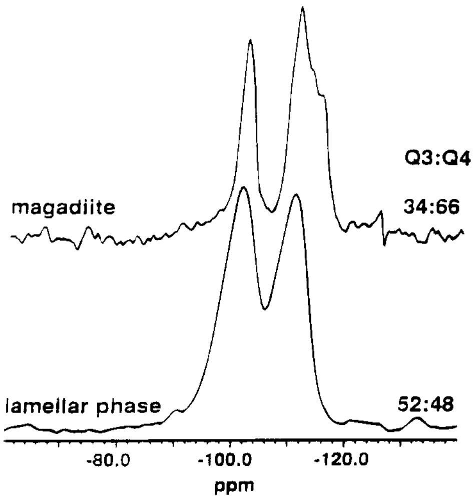

Figure 11. ^{29}Si NMR of (A) magadiite and (B) CTMA lamellar product.

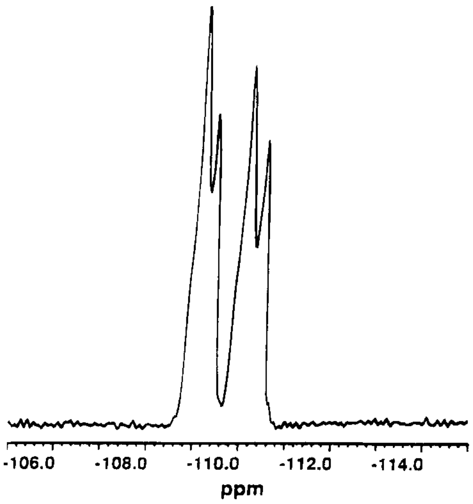

Figure 12. ^{29}Si NMR of Q8M8 product from cubic octamer.

hydrophobic ends of the surfactant molecules face one another. Any silicate structure produced from this liquid-crystal phase would be similar to that of two dimensional layered materials such as magadiite or kenyaite. However, the lack of any observable peaks in the XRD pattern of the lamellar material in the region of 20–25° 2θ suggests that these silicate layers of this lamellar phase are not as well ordered as those of layered silicates. This lack of order may be due to the higher concentration of silanol groups resulting in less condensation of the silicate species as suggested by the NMR data. Removal of the surfactant from between the silicate sheets could result in a condensation of the layers, collapsing any structure and forming a dense phase with little structural order or porosity.

Cubic Octamer. Stabilized silicate octamers have been prepared using other quaternary ammonium compounds.[28–38] They have been characterized by IR,[28] Raman,[29] X-ray diffraction,[30] and NMR.[31,32] All these materials share a double four ring (D4R), $Si_8O_{20}{}^{8-}$, with the quaternary ions functioning to stabilize the structure. There has been speculation that these double four-ring, D4R, silicate structures are precursors or secondary building units, SBU, for the formation of zeolites.[33–38] However, their hydrothermal stability is poor. For example, the tetramethylammonium cubic octamer is unstable above about 80 °C,[28,34,35] suggesting it is probably not an intermediate in the formation of crystalline materials synthesized at temperatures >100 °C and at relatively high concentrations of alkali metal ions.[39] Because milder synthetic conditions are required for the formation of M41S materials, the cetyltrimethylammonium octamer version could be an intermediate in the formation of these mesoporous molecular sieves. Figure 1d illustrates the X-ray diffraction pattern of the octamer formed in the CTMA system.

Elemental analysis agrees reasonably well with a hydrate with 4.5 H_2O associated with each CTMA. This is consistent with literature results for other tetraalkylammonium D4R species. The tetramethylammonium compound, for example, crystallizes with 8.6 H_2O/TMA.[33]

The trimethylsilylated derivative, referred to in the literature as "Q8M8", was identified on the basis of its solution Si NMR shift and its distinctive five-line solid-state Si NMR spectrum[33] (12.08, −109.12, −109.36, −110.10, and −110.47 ppm), Figure 12. The multiple Q4 peaks arise from crystallographic splitting of the otherwise identical silicons. The crystal is triclinic.[33]

A hydrothermal stability kinetic study was carried out in an NMR tube in situ at 99.8 °C in the NMR probe in parallel with steambox experiments. In agreement with literature observations, most notably the detailed studies of Knight,[31] there is slight evidence for a D4R species in the early stages and none after 24 h. The CTMA silicate octamer is stable indefinitely, in dry form or in aqueous solution, at room temperature, but decomposes in the synthetic reactant mixture at above 70 °C, suggesting that it is an unlikely intermediate in the formation of M41S structures.

Both the as-synthesized CTMA cubic octamer (Figure 13) and Q8M8 (Figure 13, insert) showed a distinct absorption band in the infrared near 580 cm^{-1}. This band is commonly found in zeolites which possess SBUs such as D4R.[40] This band has been recently assigned to an internal O−Si−O vibration using normal coordinate in the highly symmetric H form of the cubic octamer.[41,42] In addition to the Na and H forms of the

---

(28) Groenen, E. J. J.; Emeis, C. A.; van den Berg, J. P.; de Jong-Versloot, P. C. *Zeolites* **1987**, *7*, 474–77.

(29) Dutta, P. K.; Shieh, D. C. *J. Raman Spectrosc.* **1985**, *16*, 312.

(30) Smolen, Y. U. In *Soluble Silicates*; Falcone, Jr., J. S., Ed.; ACS Symposium Series 194, 1982, American Chemical Society: Washington, D. C.

(31) Harris, R. K.; Knight, C. T. G. *J. Mol. Struct.* **1982**, *78*, 273–78.

(32) Hasegawa, I.; Sakka, S. *Chem. Lett.* **1988**, 1319–22.

(33) Hoebbel, V. D.; Wieker, W. *Z. Anorg. Allg. Chem.* **1971**, *384*, 43–52.

(34) Engelhardt, G.; Hoebbel, D. *Z. Chem.* **1983**, *23*, 33.

(35) Ray, N. H.; Plaisted, R. J. *J. Chem. Soc., Dalton Trans.* **1983**, 475–81.

(36) Knight, C. T. G.; Kirpatrick, R. J.; Oldfield, E. *J. Chem. Soc., Chem. Commun.* **1986**, 66–67.

(37) Groenen, E. J. J.; Kortbeek, A. G. T. G.; Machay, M.; Sudmeijer, O. *Zeolites* **1986**, *6*, 403–11.

(38) Boxhoorn, G.; Sudmeijer, O.; van Kasteren, P. H. G. *J. Chem. Soc., Chem. Commun.* **1983**, 1416–1418.

(39) Knight, C. T. G. *Zeolites* **1990**, *10*, 140–144.

(40) Flanigen, E. M.; Khatami, H.; Syzanti, A. In *Adv. Chem. Series*; Gould, R. F., Ed.; American Chemical Society: Washington DC, 1971; p 210.

(41) Bornhauser, P.; Calzaferri, G. *Spectrochim. Acta* **1990**, *46A*, 1045.

(42) Bärtsch, M.; Bornhauser, P.; Bürgy, H.; Calzaferri, G. *Spectrochim. Acta* **1991**, *47A*, 1627–29.

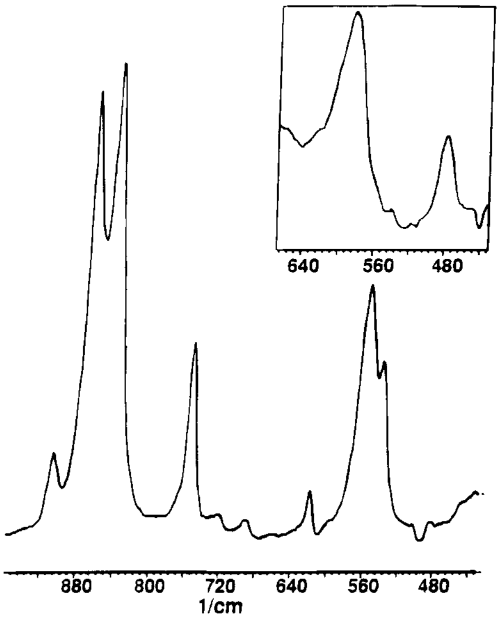

Figure 13. FTIR spectra of (A) as-synthesized CTMA cubic octamer and (B) (insert) recrystallized Q8M8 structure.

cubic octamer,[43] similar bands were reported in the tetramethylammonium silicates.[28,30-37]

CTMA silicate did lose the absorption band near 580 cm^{-1} when the FTIR sample was prepared as a pellet in a KBr matrix. A polyethylene matrix, however, gave satisfactory results. The trimethylsilylated derivative showed the band near 580 cm^{-1} even in the KBr matrix. These results seem to indicate that potassium ion exchange of the CTMA cation during mulling with solid KBr caused collapse of the D4R structure. This is consistent with the known sensitivity of the cubic octamer to the type and concentration of ammonium counterions.[44]

No absorption band in the "quartz gap" (500–650 cm^{-1}) was found for any of the M41S materials. This suggests that symmetric frameworks such as the D4R structure are not present in M41S materials and is consistent with the NMR data, which indicate that the octamer is unstable at typical M41S synthesis temperatures.

Mechanistic Considerations. The products formed in this simple synthesis system support the basic proposed liquid-crystal templating mechanism for the formation of M41S type materials. Three of the products, MCM-41 (hexagonal), MCM-48 (cubic), and the lamellar material mimic known liquid-crystal surfactant phases. The lack of stability of the cubic octamer at M41S synthesis temperatures make this compound an unlikely intermediate. The absence of any basic structural units in either NMR or FTIR analyses support this conclusion. However, the presence of this organosilicate and its stability, relative to other quaternary silicate structures, suggests that there exists a high affinity of the surfactant molecule for the silicate species. These data and the fact that MCM-41, MCM-48, and the lamellar phase can be formed in the same synthesis system by varying the silica concentration strongly support the proposed pathway B, in which the silicate anions (counterions) influence the formation of the various liquid-crystal templates.

Table 5. Effect of Various Anions on the Formation of Liquid-Crystal Phases for the Cetyltrimethylammonium System at 25 °C[a]

	wt % surfactant		
anion	hexagonal	cubic	lamellar
Cl^-	40–70	70–80	>80[a]
Br^-	20–65	>80[a]	>80[a]
$\mathrm{SO_4}^{2-}$	50–65	40–45	

[a] T = >40 °C.

The ability of various counterions to influence the formation of liquid-crystal phases in surfactant systems is well documented in the literature. Variation in the counterion can influence whether a given liquid-crystal phase will form and at what surfactant concentration. The data presented in Table 5 illustrates the effect of different anions on the formation of liquid-crystal phases for the cetyltrimethylammonium system at 25 °C. For example, the hexagonal phase is favored over a wider and lower concentration range for the bromide containing system than for the chloride containing system.[16,46] The cubic phase forms in the sulfate-containing system at lower surfactant concentration than the hexagonal phase.[47] In a similar fashion, we believe that the silicate anions present in the M41S type preparations influence the formation of the various M41S phases that mimic known liquid-crystal phases. However, for the silicate system, these phase formations take place at relatively low surfactant concentration (~20–26 wt %). In the case of the silicate containing system, the anion (silicate) has the ability to form extended oligomers that result in the formation of stable inorganic structures MCM-41 (hexagonal), MCM-48 (cubic), and the lamellar phase.

The presence of alcohol is known to disrupt the formation of liquid-crystal phases in CTMA-containing solutions.[47] Ethanol can disrupt the hexagonal liquid-crystal phase at weight percentages of between 10 and 40% depending on the amount of surfactant in solution (~30–60%). However, in the M41S silicate/surfactant system, ethanol, generated in situ by the hydrolysis of TEOS, apparently does not have the same effect. For the MCM-41 preparation, the amount of ethanol generated could be as high as 50 wt % based on 4 mol of ethanol/mol of TEOS. In fact, all three liquid-crystal phases, hexagonal, cubic, and lamellar, were formed in the presence of potentially substantial amounts of ethanol. This may suggest that the silicate precursor responsible for the formation of the M41S structures is formed quite rapidly and is unresponsive to subsequent solution chemistry changes.

The sequence in which the phases are formed in this system is also consistent with a liquid-crystal templating mechanism. In surfactant chemistry, the hexagonal phase is typically the most stable and is formed with the least amount of perturbation of the system. Only

---

(43) Borbely, G.; Beyer, H. K.; Karge, H. G.; Schweiger, W.; Brandt, A.; Bergk, K.-H. *Clays Clay Miner.* **1991**, *39*, 490.

(44) Benn, R.; Grondey, H.; Brevard, C.; Pagelot, A. *J. Chem. Soc., Chem. Commun.* **1988**, 102–104.

(45) For a normal-coordinate analysis treatment of this region in zeolites see: van Santan, R. A.; Vogel, D. L. *Advances in Solid State Chemistry*; JAI Press: Greenwich, CT, 1989; p 151.

(46) Henriksson, U.; Blackmore, E. S.; Tiddy, G. J. T.; Soderman, O. *J. Phys. Chem.* **1992**, *96*, 3894–3902.

(47) Fontell, K.; Khan, B.; Lindstrom, K. B.; Maciejewska, D.; Puang-Ngern, S. *Colloid Polym. Sci.* **1991**, *269*, 727–42.

when the surfactant concentration, or other additives, are in greater concentration do the cubic and lamellar phases form.[15] In the M41S system, MCM-41 is formed with the highest concentration of silica, i.e., lowest Sur/Si ratio. The other two phases are formed at progressively higher Sur/Si ratios. Since the surfactant concentration for this system is below the concentration, where liquid-crystal structures typically appear,[4] pathway B seems a likely route for the formation of these new materials.

Recently, Monnier et al.[25] and Chen et al.[48] have explored the details of the liquid-crystal templating mechanism we first proposed.[1,3] These workers suggest that the precursor to the hexagonal member of the M41S family is either a lamellar phase[25] or a collection of individually silicated surfactant rods.[48] In both of these proposed mechanisms, the intermediates are silicate clad structures which are consistent with the proposed silicate initiated pathway. The transformation from a lamellar precursor to the hexagonal MCM-41 structure proposed by Monnier et al. appears plausible.[25] However, the transformation from this layered semicondensed silicate structure to a multidimensional structure for the cubic phase is more difficult to envision, unless this transformation from the lamellar phase to the hexagonal or cubic phase occurs quite rapidly and involves essentially bilayers of silicate/surfactant species. Both the cubic structure (i.e., bicontinuous) and a lamellar structure could be constructed from a bilayer precursor to represent the appropriate liquid-crystal phases and their M41S counterparts.

The formation of hexagonal, cubic, and lamellar structures using the proposed individual silicated surfactant rods also appears feasible.[48] As stated earlier, one of the proposed structures of the cubic liquid-crystal phase consists of intertwined surfactant rods.[20] A lamellar structure could also be constructed by stacking these same silicated rods directly on top of each other (a slight variation from the hexagonal packing needed for the MCM-41 formation). In either proposed intermediate, it is a silicated species that is responsible for the formation of the M41S structures, and there are subtle reaction variables responsible for the transformation between the three isolated phases (hexagonal, cubic, and lamellar). Our work suggests that this transformation is highly dependent on the surfactant to silica ratio, namely, at Sur/Si molar ratio <1 the hexagonal phase is made directly. At slightly higher values (Sur/Si 1−1.5), the cubic phase is obtained; at Sur/Si 1.2−2 the lamellar phase dominates.

Conclusions

The surfactant-to-silica molar ratio is a critical variable in the formation of liquid-crystal templated M41S materials. As this ratio was increased from 0.5 to 2.0, the siliceous products exhibited XRD patterns that are consistent with liquid-crystal phase transformations. These products exhibit hexagonal, cubic, and lamellar structures which mimic well-known liquid-crystal phases. The formation of these structures support the proposed mechanistic pathway in which M41S type materials form via a silicate anion induced liquid-crystal phase. Although the cubic octamer was also isolated in this same synthetic system, its lack of thermal stability at synthesis temperatures used for the formation of M41S materials suggest that this D4R structure is an unlikely intermediate or building unit of the silicate wall.

Acknowledgment. The authors are grateful to the staff at Mobil's Central and Paulsboro Research Laboratories for their invaluable discussion and effort. In particular, we acknowledge C. D. Chang, R. M. Dessau, and H. M. Princen for alerting us to references in the surfactant literature and helpful discussions on surfactant liquid crystal phases. We thank S. L. Laney, N. H. Goeke, H. W. Solberg, J. A. Pearson, and C. Martin for their expert technical assistance and J. B. Higgins for helpful technical discussions. We also thank Mobil Research and Development Corp. for its support.

---

[48] Chen, C. Y.; Burkett, S. L.; Li, H. X.; Davis, M. E. *Microporous Mater.* **1993**, *2*, 27−34.